Available online at www.sciencedirect.com
ScienceDirect
International Journal of Pharmaceutics 355 (2008) 314–320
INTERNATIONAL JOURNAL OF PHARMACEUTICS
www.elsevier.com/locate/ijpharm

Pharmaceutical Nanotechnology

Solid lipid nanoparticles of temozolomide: Potential reduction of cardial and nephric toxicity

Guihua Huang [a,*], Na Zhang [a], Xiuli Bi [a], Mingjin Dou [b]

[a] *Pharmaceutical College, Shandong University, 44 Wen hua Xi Lu, Ji'nan250012, Shandong Province, PR China*
[b] *Department of Pharmacy,Shandong Province Tumour Hospital, Ji'nan 250013, PR China*

Received 2 July 2007; received in revised form 19 November 2007; accepted 15 December 2007
Available online 23 December 2007

Abstract

The aim of this study was to prepare temozolomide solid lipid nanoparticles (TMZ-SLNs), to evaluate its physiochemical characteristics, and to investigate the specific drug targeting of intravenous (i.v.) injected solid lipid nanoparticles of temozolomide. TMZ-SLNs was prepared by an emulsification and low-temperature solidification method. *In vitro* drug release was conducted in phosphate-buffered saline (pH 6.8) at 37 °C. The concentrations of the temozolomide in selected organs were determined using reversed-phase high-performance liquid chromatography (HPLC) following i.v. administration of the TMZ-SLNs and a temozolomide solution (TMZ-Sol). The results show that the TMZ-SLNs had an average diameter of 65.9 ± 11.8 nm with a zeta potential of −37.2 ± 3.6 mV and the *in vitro* drug release was monitored for up to 3 days, and the release behavior was in accordance with Higuchi-equation. In the tested organs, the AUC/dose and the mean residence times (MRT) of the TMZ-SLNs were much higher and longer than those of the TMZ-Sol, especially in brain and reticuloendothelial cells-containing organs. The AUC ratio of TMZ-SLNs to TMZ-Sol in the brain was the highest among the organs. These results indicated that the SLNs is a promising sustained-release and drug-targeting system for antitumor drugs. It may also allow a reduction in dosage and a decrease in systemic toxicity.

Keywords: Solid lipid nanoparticles; Temozolomide; Body distribution; Drug targeting; Sustained release system

1. Introduction

Nanoparticles made from solid lipids, which are in the submicron size range (50–1000 nm) and composed of physiological lipids, have caught increasing attentions as colloidal drug carriers for intravenous (i.v.) application (Muller et al., 2000; zur Muhlen et al., 1998; Cavalli et al., 1995; Yang et al., 1999). At room temperature the particles are in the solid state so the mobility of incorporated drugs, a prerequisite for controlled drug release, is greatly reduced. They can be stabilized by non-toxic surfactants, such as Poloxamer and lecithin (Muller et al., 1996). *In vitro* tests show that temozolomide-loaded solid lipid nanoparticles (SLNs) may be suitable as a drug–carrier system for potential i.v. use because of its relatively low cytotoxicity compared to polymeric nanoparticles (Muller et al., 1996, 1997). SLNs possess the characteristics of no burst release when it was obtained with fat emulsions. *In vitro* release of prednisolone as reported may last for up to 6 weeks (Muller et al., 1995). Colloidal drug carriers, such as nanoparticles, have been shown to accumulate in the reticuloendothelial system (RES). In addition to the ability to accumulate in the RES, it has been demonstrated that nanoparticulate uptake in the RES can be influenced by altering the surface properties of the nanoparticles (Couvreur et al., 1995).

Alkylating agents play an important role in the treatment of intracalvarium spongioblastoma and malignant tumors of the nervous system in human. Among them, temozolomide has shown significant effects against a wide range of human cancers (Newlands et al., 1992, 1997). Unfortunately, the use of temozolomide in clinics is restricted by an unusual cardiomyopathy, which is caused by the accumulation of this drug. In addition, temozolomide also produces acute toxicity, such as bone marrow depression and oral ulcerations (Du, 2000). To avoid treatment-limiting side effects and to get better efficacy, modern therapy requires that the drug reaches the site of action in the most efficient way, which can be achieved, by using colloidal drug carriers as delivery system (Yang et al., 1999),

* Corresponding author at: The Pharmaceutical College, Shandong University, , China. Tel.: +86 531 88382015; fax: +86 531 82983991.
E-mail address: hgh2003@126.com (G. Huang).

0378-5173/$ – see front matter © 2007 Elsevier B.V. All rights reserved.
doi:10.1016/j.ijpharm.2007.12.013

such as microemulsions, liposomes, niosomes and polymeric nanoparticles.

In the present work, we reported the encapsulation of temozolomide using SLNs as the drug carrier. SLNs as colloidal drug carriers combined the advantages of polymeric nanoparticles and liposomes while simultaneously avoiding some of their disadvantages such as acute and chronic toxicity or low stability (Muller et al., 2000). In addition, this study aimed to achieve controlled release of temozolomide, meanwhile avoiding adverse side effects by the conventional formulation. The use of nanoparticles as the drug–carrier system is a very attractive strategy to achieve controlled drug release (Allen and Cullis, 2004). A distinct advantage of SLNs over polymeric nanoparticles is the fact that the lipid matrix is made from physiologically tolerated lipid components, which decreases the potential acute and chronic toxicity. We aimed to examine if temozolomide carried by SLN shows a different pharmacokinetic behaviour in comparison to the temozolomide solution (TMZ-Sol) currently widely used in chemotherapy. We also aimed to develop a new delivery system of temozolomide to reduce toxicity and side effects.

2. Materials and methods

2.1. Materials

Pure lecithin of medical grade was purchased from Shanghai Biology Technology Co. Ltd. (Shanghai, China); Poloxamer188 of medical grade, from Sigma Co. (Germany); temozolomide from the Laboratory of Chemistry Institution of Shandong University (Jinan, China); Tween 80, from Tianjin Tianda Chemical Industry. All chemicals were either analytical or spectroscopic grade. Distilled water was filtered through a 0.45-μm (cellulose acetate) membrane prior to use.

2.2. Optimization of prescription and technology with orthogonal experimental design

Based on the investigation of single factor, four factors which mainly affected entrapment efficiency, were chosen as research objects such as (*A*) the ratio of lecithin to stearic acid (w/w); (*B*) the ratio of drug to stearic acid (w/w); (*C*) time of emulsification (*h*); and (*D*) the concentration of Poloxamer188 (w/v). Nine pieces of prescriptions were designed according to L_9 (3^4) orthogonal experimental design, in order to screen optimal, formulations of prescription and artwork of preparation. Based on entrapment efficiency as evaluation index, the factors and levels of the orthogonal experimental design were listed in Table 1.

2.3. Preparation of TMZ-SLNs

Temozolomide (8 mg) was dissolved in 1 ml of hydrochloric acid (0.1 mol/l), and mixed with 5 ml of acetone solution containing 80 mg of stearic acid and 10 mg lecithin. The mixtures was sonicated, and was then added to 50 ml 0.8% (w/v) of Poloxamer188 solution, stirring (Heracus Co. Germany) at 2000 rpm for 0.5 h. The mixed solution was transferred to icy water bath (about 0–2 °C) for 4.0 h and continuously stirred in order to form SLNs (Manjunath and Venkateswarlu, 2005). The TMZ-SLNs suspension was either stored at 4 °C or lyophilized for long-term storage. The generating and storage of the TMZ-SLNs was conducted under nitrogen atmosphere.

Table 1
Factor and level of the orthogonal experiment design

Levels	Factors			
	A (g/g)	*B* (g/g)	*C* (h)	*D* (%) (g/ml)
1	1:4	1:5	0.5	0.8
2	1:8	1:8	2.0	1.6
3	1:20	1:10	4.0	2.4

A: ratio of lecithin to stearic acid (w/w); *B*: ratio of drug to stearic acid (w/w); *C*: time of emulsification (h); *D*: concentration of Poloxamer188 (w/v).

TMZ-Sol (10 mg/ml) was prepared by dissolving 0.5 g of temozolomide in a 50 ml of the solution containing 30% (w/v) of 2-hydroxypropyl-β-cyclodextrin (2-HP-β-CD, Shanxi Liquan Drug Co. Ltd.) at 35 °C in water bath by stirring at 800 rpm for 1.0 h.

2.4. Physicochemical characterization of SLNs

The morphology and average diameter of TMZ-SLNs was examined by transmission electron microscopy (JEM-1200EX, Japan). The zeta potential of the TMZ-SLNs suspension was measured by the electrophoretic mobility of the nanoparticles in a U-type tube at 20 °C.

2.5. Determination of drug loading and entrapment efficiency

The TMZ-SLNs suspension (100 ml) was acidified to pH 1.2 with 1 mol/l HCl producing aggregation of the SLNs and the admixture solution was immediately separated by centrifugation using ultracentrifugation (40,000 rpm for 30 min, Heracus Co., Germany). The concentrations of temozolomide in TMZ-SLNs supernatant were measured after dilution by HPLC. The entrapment efficiency (EE) of temozolomide in SLNs was also determined using the following equation:

$$\mathrm{EE}\,(\%) = 1 - \frac{\text{amount of drug in supernatants}}{\text{amount of drug added}} \times 100 \qquad (1)$$

Drug loading was calculated as drug analyzed in the nanoparticles versus the total amount of the drug and the excipients added (lecithin, stearic acid and Poloxamer188) during preparation according to following equation:

$$\mathrm{DL}\,(\%) = \frac{\text{amount of drug in precipitations}}{\text{amount of drug added} + \text{amount of excipients added}} \times 100 \qquad (2)$$

2.6. Evaluation of in vitro release

In vitro release was evaluated by using a dialysis bag diffusion technique (Yang et al., 1999). The TMZ-SLNs suspension

was placed in dialysis bags with a 12,000 molecular weigh cut-off (Sigma) and immersed in 200 ml phosphate-buffered saline (pH 6.8) at 37 °C by using a RC Drug Dissolution Tester (Tianjin Medical Instrumental Factory, Tianjin, China) with paddle rotating at 100 rpm. An aliquot of 0.5 ml dissolution medium was removed at a series of various points (1, 2, 6, 8, 12, 24, 36, 48, 60 and 72 h) and the same volume of fresh dissolution medium was added accordingly. The aliquots were diluted with mobile phase prior to the analysis by HPLC.

2.7. Pharmacokinetics and tissue distribution

Six healthy rabbits (provided by Center of Experimental Animal, Shandong University, body weight 2.5 ± 0.5 kg, three females and three males) were used for pharmacokinetics studies. The rabbits were fasted overnight with free access to water. The TMZ-SLNs suspension containing temozolomide 10 mg/kg body weight and the TMZ-Sol was injected intravenously into the ear vein of rabbits. One milliliter of blood samples were drawn after the injection of TMZ-Sol at time 0, 0.25, 0.5, 1, 2, 4, 6, 8 and 12 h, or after the injection of TMZ-SLNs at time 0, 0.25, 0.5, 1, 2, 4, 6, 8, 12, 24, 36 and 48 h. Blood samples were collected in heparinized tubes, and centrifuged at 2000 rpm for 15 min. Plasma tubes were snap-frozen and stored at −20 °C until use.

The mixture of containing 0.4 ml of plasma and 2 ml of acetone was vortexed for 5 min and then centrifuged at 4000 rpm for 15 min. An aliquot of the supernatant (1 ml) was evaporated under nitrogen at 60–70 °C before the residue was reconstituted in 200 μl of mobile phase before the analysis by HPLC.

Kunming mice (provided by Center of Experimental Animal, Shandong University, body weight 20 ± 1.0 g, female or male) were used for body distribution studies. The mice were fasted overnight with free access to water. The TMZ-SLNs suspension and the TMZ-Sol were injected intravenously into the tail vein of the mice. For each preparation and each sampling time point, 3 mice were treated with a single dose of 10 mg of TMZ/kg after the injection of TMZ-Sol at time 0, 0.25, 1, 2, 4, 6, 8 and 12 h or after the injection of TMZ-SLNs at time 0, 0.25, 1, 2, 4, 6, 8, 12, 24 and 48 h. The mice were sacrificed and selected organs, liver, heart, lung, kidneys, brain and spleen were dissected. Tissues tubes were snap-frozen and stored at −20 °C until use.

Each organ sample was weighed and homogenized before 2 ml of acetone was added to 0.4 ml of homogenate and the mixture was vortexed for 5 min and then were centrifuged at 4000 rpm for 15 min. An aliquot of the supernatant (1 ml) was evaporated under nitrogen at 60–70 °C before the residue was reconstituted in 200 μl of mobile phase before the analysis by HPLC.

2.8. HPLC analysis of temozolomide

Concentrations of temozolomide were measured by the method of reversed-phase HPLC. And analytical column was AichromBond-1 C_{18} column (4.6 mm × 250 mm). Temozolomide was monitored at a wavelength of 329 nm. The mobile phase was composed of methanol (spectroscopic grade) containing 0.5% of glacial acetic acid solution (10:90) at a flow rate of 1.0 ml/min. Plasma, blood and homogenized tissue samples were precipitated with acetone and vortexed for 5 min. After centrifugation, the clear supernatant of the blood and plasma was immediately chromatographed, and the tissue samples were stored at −20 °C before the analysis. Aliquots of supernatants (20 μl) were loaded on the HPLC. The detection limit of temozolomide was 10 ng/ml intraday and interday variabilities were 3 and 5%, respectively. Mean recovery rates of each organ exceeded 80%, R.S.D. < 8%.

2.9. Data analysis

Plasma and tissue concentrations data of temozolomide obtained from rabbits and mice were pooled to provide mean concentrations. Pharmacokinetic parameters in plasma and tissue were calculated by using a statistical moment algorithm (Drug and Statistics by DAS program (Dept. Clinical pharmacology, Shandong Qilu Hospital, Jinan, China). The area under the concentration–time curve (AUC) and the area under the first moment curve (AUCM) was calculated using the linear trapezoidal rule. Mean residence time (MRT) and bioavailability value (F) was defined as follows

$$\mathrm{MRT} = \frac{\mathrm{AUMC}}{\mathrm{AUC}} \quad \text{and} \quad F = \frac{(\mathrm{AUC})_{\mathrm{TMZ\text{-}SLN}} \times \mathrm{dose}_{\mathrm{TMZ\text{-}Sol}}}{(\mathrm{AUC})_{\mathrm{TMZ\text{-}Sol}} \times \mathrm{dose}_{\mathrm{TMZ\text{-}SLN}}}$$

3. Results and discussion

3.1. Orthogonal experimental design

The orthogonal experimental design was in Table 2.

The range reflected the extent of each factor affecting on index and range was bigger, extent affected was greater. Four factors in the present experiment were arranged as $A > B > D > C$. On the basis of synthetic mean value, the optimized level combination of every factor was chosen. The bigger synthetic mean value,

Table 2
Result of orthogonal experiment and direct-viewing analyses

Experiment number	*A*	*B*	*C*	*D*	*P*
1	1	1	1	1	50.70
2	1	2	2	2	25.00
3	1	3	3	3	52.23
4	2	1	2	3	40.64
5	2	2	3	1	48.29
6	2	3	1	2	58.58
7	3	1	3	2	17.81
8	3	2	1	3	28.46
9	3	3	2	1	40.46
K_1	127.93	109.15	137.74	139.45	
K_2	147.51	107.75	106.10	101.39	
K_3	86.73	151.27	118.33	121.33	
K_{11}	42.64	36.38	45.91	46.48	
K_{12}	49.17	33.92	35.37	33.80	
K_{13}	28.91	50.42	39.44	40.44	
R	20.26	16.50	10.54	12.68	

A: ratio of lecithin to stearic acid (w/w) *B*: ratio of drug to stearic acid (w/w) *C*: time of emulsification (h) *D*: concentration of Poloxamer188 (w/v).

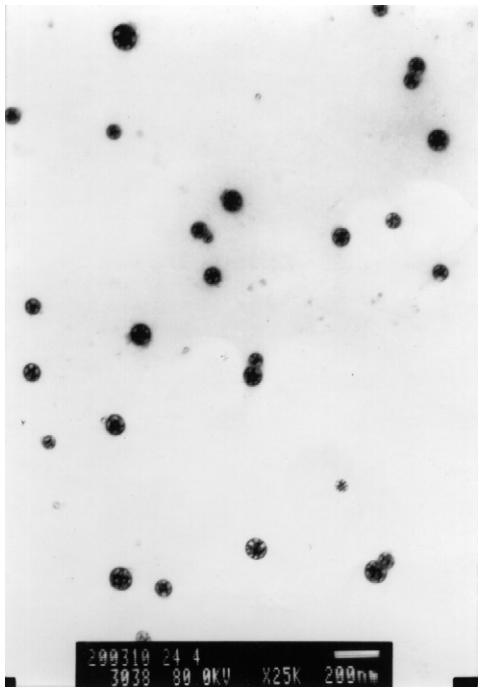

Fig. 1. Microphotograph of TMZ-SLNs by transmission electron microscope ($\times 10^6$).

the better the level was. The best experimental combination was made by the optimal level of every factor combined. Analytic results of four factors were, *A*: 2 > 1 > 3; *B*: 3 > 1 > 2; *C*: 1 > 3 > 2; *D*: 1 > 3 > 2 and optimized combination was $A_2B_3C_1D_1$, i.e., lecithin/stearic acid (1:8, g/g), drug/stearic acid (1:10, g/g) and dosage of Poloxamer188 (0.8%, g/ml). Preparation artwork: emulsification time (0.5 h), emulsification temperature (60 °C), stirring speed (2000 rev/min) and temperature of ice bath (0–2 °C).

3.2. Nanoparticles characterization

Under transmission electron microscopy, a dense sphere pattern with an average diameter of 65.9 ± 11.8 nm ($n = 3$) (Fig. 1) and non-normal distribution (Fig. 2) was observed for freshly prepared TMZ-SLN samples. The surface carried negative charges with a zeta potential of −37.2 ± 3.6 mV ($n = 3$).

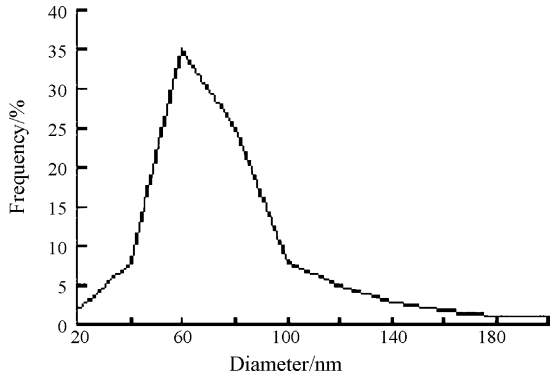

Fig. 2. Size distribution of TMZ-SLNs.

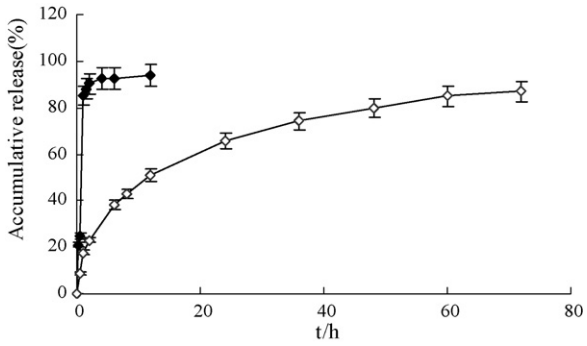

Fig. 3. The releasing curve of TMZ-Sol (♦) and TMZ-SLNs (◊) in PBS (pH 6.8).

Drug loading was 0.946 ± 0.019% ($n = 3$), and the entrapment efficiency was 58.9 ± 1.2% ($n = 3$).

3.3. Evaluation of in vitro release

In *in vitro* release experiments, dynamic dialysis was chosen for separation of free drug from drug-incorporated nanoparticles. Fig. 3 shows the temozolomide release from the TMZ-Sol and the TMZ-SLNs in phosphate-buffered saline (pH 6.8) at 37 °C. The result indicated the release of temozolomide from TMZ-Sol was very quick. Approximately 85.2% of the drug had been released after 1 h. On the contrary, the release of temozolomide from SLNs was very slow and 17.6% of releases from TMZ-SLNs were measured within 1 h, followed by a slower and continuous release. By 72 h the total release from the TMZ-SLNs was 87.3%. The SLNs could reduce temozolomide release. Drug release data from the TMZ-SLNs was fitted to Higuchi equations. $Q = 0.1038\, t_{1/2} + 0.0944$ ($\gamma = 0.9915$). The time of 50% drug released was 15.27 h and 63.2% of drug released was 26.82 h.

3.4. Pharmacokinetics and tissue distribution

Plasma concentration–time data of the TMZ-SLNs and the TMZ-Sol was analyzed by using DAS program. Pharmacokinetic parameters are shown in Table 3 and mean plasma

Table 3
The comparative plasma pharmacokinetic parameters after i.v. 10 mg/kg administration of TMZ-Sol and of TMZ-SLNs in rabbits ($n = 6$)

Parameter	TMZ-Sol	TMZ-SLN
α (h^{-1})	1.70	1.26
β (h^{-1})	1.18	0.024
$t_{1/2\alpha}$ (h)	0.41	0.55
$t_{1/2\beta}$ (h)	3.96	29.23**
k21 (h^{-1})	0.48	0.22
k10 (h^{-1})	0.50	0.014
k12 (h^{-1})	2.93	0.46
MRT (h)	3.78	45.32**
AUC (h ng ml^{-1})	807.63	7305.67**
C_{max} (ng ml^{-1})	376.2	200.1
CL (mg kg^{-1}/h ng ml^{-1})	0.0124	0.0014**

** $P < 0.001$.

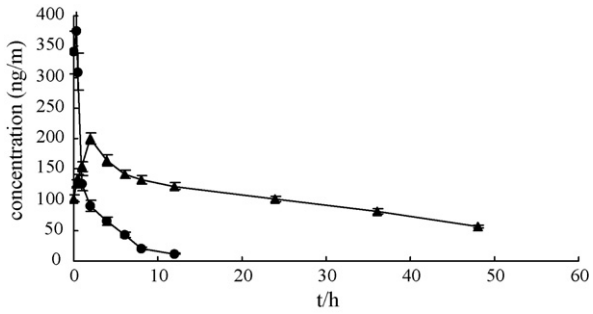

Fig. 4. Plasma concentration *vs.* time for 10 mg kg^{-1} of TMZ-Sol (●) and TMZ-SLNs (▲).

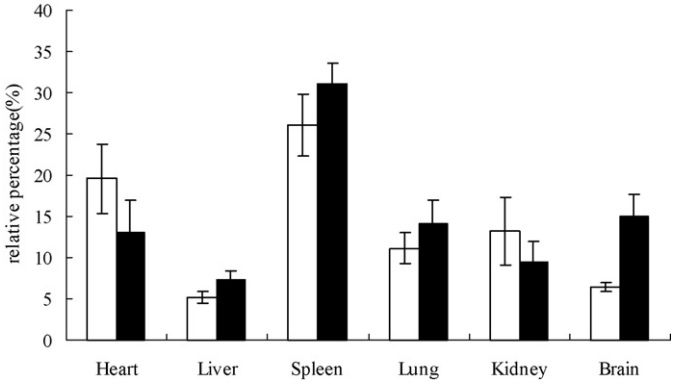

Fig. 5. Tissue distribution of TMZ after i.v. administration of TMZ-SLNs (■) and TMZ-Sol (□) in mice.

concentration–time curves of the TMZ-SLNs and the TMZ-Sol after intravenous administration were shown in Figs. 4 and 5 shows AUC/dose in various organs after 12 h. Compared to the TMZ-Sol, targeting efficiency was increased in liver, spleen, lung and brain, but significantly decreased in heart and kidney when TMZ entrapped in SLNs were administered intravenously. AUC/dose, MRT and *F* values of tested organs were given in Table 4. Body distribution experiment in mice indicated that comparing to the TMZ-Sol, targeting efficiency of the TMZ-SLNs was significantly increased in brain. Plasma concentration–time curves of the brain were given in Fig. 6.

In this study, the TMZ-SLNs and the TMZ-Sol were intravenously administered to rabbits. Plasma temozolomide levels reached minimum within 12 h, whereas plasma temozolomide levels were observed up to 48 h after administration of SLNs. Following i.v. administration of the TMZ-Sol, the mean measured peak plasma concentration achieved was 376.2 ng/ml and with TMZ-SLNs it was 200.1 ng/ml. After intravenous administration of the TMZ-SLNs, free temozolomide was available

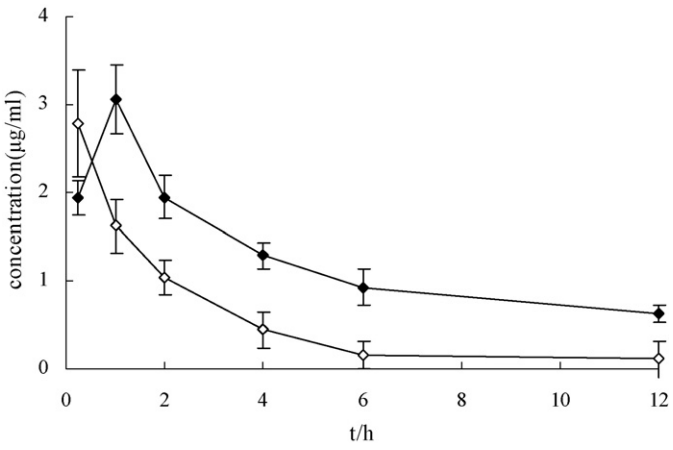

Fig. 6. Brain concentration–time curves of TMZ after i.v. administration. TMZ-SLNs (♦) and TMZ-Sol (◊) with the same dose of 10 mg/kg in mice ($n = 5$).

for solvation and might have dissolved in plasma. Subsequently, solution of temozolomide distributed rapidly, compared to distribution of temozolomide entrapped in solid lipid nanoparticles (Manjunath and Venkateswarlu, 2005). The initial plasma concentration (at 2 h) was lower for the TMZ-SLNs than the TMZ-Sol following intravenous administration, possibly because temozolomide was released slowly from SLNs for extended period of time and free drug was available for distribution only after its release. After 2 h, the plasma concentration was lower for the TMZ-Sol than that of the TMZ-SLNs because of its solubility in plasma ensuing rapid distribution, elimination and slower release of temozolomide from SLNs leading to lower clearance.

Plasma kinetics of temozolomide shown in Table 3 with a higher AUC and lower rates of clearance may to due to slower distribution of temozolomide incorporated in SLNs than that of TMA-Sol. From Table 3, we can see that the AUC increased from 807.6 h ng ml^{-1} for the TMZ-Sol to 7305.67 h ng ml^{-1} for the TMZ-SLNs with corresponding decrease of the clearance from 0.0124 to 0.0014 mg kg^{-1}/h ng ml^{-1}. Increased MRT values of the TMZ-SLNs than that of TMZ-Sol were observed (Table 3). Increased MRT values were due to the presence of Poloxamer188 on the surface of nanoparticles and the slow release of temozolomide from the SLNs (Manjunath and Venkateswarlu, 2005). This observation supports by some previous studies. MRT of camptothecin SLNs increased around 18 times to solution of camptothecin administered intravenously (Yang et al., 1999). Polystyrene nanoparticles coated with Poloxamer188 and 338 showed prolonged circulation times compared to uncoated nanoparticles (Illum and Davis, 1983).

Table 4
The comparative tissue pharmacokinetic parameters after i.v. administration of TMZ-Sol and of TMZ-SLNs in mice

Sample	Parameter	Heart	Liver	Spleen	Lung	Kidney	Brain
TMZ-SLN	MRT (h)	2.54	1.75	2.65	3.66	2.44	4.27
	AUC (h ng ml^{-1})	12.99	7.40	31.08	14.10	9.46	15.07
	F	0.66	1.43	1.19	1.27	0.72	2.34
TMZ-Sol	MRT (h)	2.21	1.75	1.92	1.90	2.14	2.23
	AUC (h ng ml^{-1})	19.59	5.19	26.13	11.11	13.22	6.43

Fig. 6 shows that the temozolomide was present in the brain at 12 h after the administration of the TMZ-SLNs. Temozolomide's concentrations with the SLNs were higher than that of the TMZ-Sol in the brain. AUC, MRT and *F* values of tested organs were given in Table 4. MRT values for all the tissues were found higher than TMZ-Sol. AUC values with the TMZ-SLNs were higher than the TMZ-Sol in liver, spleen, lung and brain; and lower than the TMZ-Sol in heart and kidney. The highest *F* value was observed with TMZ-SLNs in brain (Table 4).

Intravenously injected particulated substances of administrated drug carriers with an average size below 7 μm are normally taken up by the macrophages of the RES, particularly by the Kupffer cells in the liver. For the organs of the RES, Table 4 shows that *F* was 1.43, 1.27 and 1.19 in liver, lung and spleen, respectively.

Higher concentrations of temozolomide and *F* value indicated that temozolomide SLNs were mainly accumulated in RES organs. Similar results were reported by Yang et al. (1999) for camptothecin SLN. The RES has a major role in removing small xenobiotic particles from the blood by coating them with serum components opsonins, which acts as labels to passively target the nanoparticles by certain phagocytic cells (Couvreur et al., 1995; Moghimi, 1995). In non-RES organs, such as brain, *F* also increased significantly. This result might be due to the sustained release of temozolomide from the TMZ-SLNs or the absorption of Poloxamer188 on the surface of TMZ-SLNs (Moghimi, 1995). Because of the hydrophilicity and steric hindrance of Poloxamer188 (Moghimi, 1995; Lenaerts et al., 1995), opsonins are less adsorbed on the nanoparticle surface, which results in lower englobement of MNP to nanoparticle and longer resistance time in blood. Targeting efficiency for serum and brain was found to be higher than that in liver, spleen and lung, which is rich in mononuclear phagocyte. The TMZ-SLNs possesses some initiative targeting characteristics that may be helpful to the therapy of lymph-cancer and brain tumor.

In non-RES organ, such as brain, *F* increased significantly. TMZ-SLNs can enhance brain concentrations of temozolomide and maintain high drug levels for up to 48 h (Fig. 6). Compared with the same dose of TMZ-Sol, the AUC/dose of TMZ-SLNs in brain was 2.34-fold greater and MRT increased 1.9 times. These results indicated TMZ-SLNs had successfully targeted temozolomide to brain and could greatly improve the efficacy of temozolomide to treat brain cancers, with a significant increase of brain targeting efficiency from 6.76 to 13.25%.

The study of lipid microspheres transport containing clinprost and Tween 80-coated nanoparticles across blood–brain barrier showed the similar mechanism. Therefore, consistent with literature, TMZ-SLNs can increase the brain targeting, which may be a result of intact TMZ-SLNs transport across the blood–brain barrier by endocytosis or by phagocytic uptake of the brain blood vessel endothelial cells. The drug could then be delivered by passive diffusion from the endothelial cells to the brain cells and generate therapeutic effects.

However, AUC values with TMZ-SLNs were lower in heart and kidney than in the TMZ-Sol (Table 4). Targeting efficiency in heart and kidney of the TMZ-SLNs was lower. After 12 h, concentrations in the heart and kidney (the main organs of associated with TMZ toxicity) of mice treated with TMZ-SLNs, respectively were 33.7% and 28.4% lower than that of mice treated with TMZ-Sol. The TMZ-SLNs can decrease renal and cardiac accumulation of the drug and reduce the toxicity and side effects on heart and kidney.

Temozolomide can produce cardiomyopathy and acute toxicity, such as in the form of bone marrow depression and oral ulcerations (Du, 2000). Because of the change in pharmacokinetics of temozolomide, such as the reduction of C_{max} and the prolongation of the time to reach C_{max}, temozolomide incorporated into SLNs shows lower toxicity than that in the TMZ-Sol. The higher MRT and *F* values in brain for the TMZ-SLNs indicated that TMZ-SLNs could greatly improve temozolomide treatment efficacy compared to the TMZ-Sol.

4. Conclusions

In vitro release tests showed that the TMZ-SLNs exhibited sustained release. Compared to the TMZ-Sol, temozolomide SLNs shows high uptake in the RES organs and brain following intravenous administration. The TMZ-SLNs can effectively target the brain by crossing the blood–brain barrier. Based on the body distribution pattern and disposition kinetics, the SLNs may be good for the targeting of anticancer drugs when effective drug concentrations in timorous tissue need to be high and last for longer time.

Acknowledgements

We are thankful to Mrs. Wu for her help in the average diameter, polydispersity index and Z-potential of the SLNs determination, and Mrs. Du for the transmission electron microscopy examination.

References

Allen, T.M., Cullis, P.R., 2004. Drug delivery systems: entering the mainstream. Science 303, 1818–1822.

Cavalli, R., Morel, S., Gasco, M.R., Chetoni, P., Saettone, M.F., 1995. Preparation and evaluation in vitro of colloidal lipospheres containing pilocarpine as ion pair. Int. J. Pharm. 117, 243–246.

Couvreur, P., Dubernet, C., Puisieux, F., 1995. Controlled drug delivery with nanoparticles: current possibilities and future trends. Eur. J. Pharm. Biopharm. 41, 2–13.

Du, X.L., 2000. Temozolomide: a new drug for the treatment of intractable and polymorphism glioma. Chin. Pharm. J. 35, 135.

Illum, S.L., Davis, S.S., 1983. Effect of the nonionic surfactant Poloxamer338 on the fate and deposition of polystyrene microspheres following intravenous administration. J. Pharm. Sci. 72, 1086–1089.

Lenaerts, V., Akbiri, L., Chouinard, F., et al., 1995. Nanocapsules with a reduced liver uptake: targeting of phthalocyanines to EMT-6 mouse mammary tumour in vivo. Eur. J. Pharm. Biopharm. 41, 38–43.

Manjunath, K., Venkateswarlu, V., 2005. Pharmacokinetics, tissue distribution and bioavailability of clozapine solid lipid nanoparticles after intravenous and intraduodenal administration. J. Control. Release 107, 215–228.

Moghimi, S.M., 1995. Mechanisms regulating body distribution of nanospheres conditioned with pluronic and tetronic block co-polymers. Adv. Drug Deliv. Rev. 16, 183–193.

zur Muhlen, A., Schwarz, C., Mehnert, W., 1998. Solid lipid nanoparticles (SLN) for controlled drug delivery-drug release and release mechanism. Eur. J. Pharm. Biopharm. 45, 149–155.

Muller, R.H., Maassen, S., Schwarz, C., Mehnert, W., 1997. Solid lipid nanoparticles (SLN) as potential carrier for human use: interaction with human granulocytes. J. Control. Release 47, 261–269.

Muller, R.H., Maassen, S., Weyhers, H., Mehnert, W., 1996. Phagocytic uptake and cytotoxicity of solid lipid nanoparticles (SLN) sterically stabilized with Poloxamine908 and Poloxamer407. J. Drug Target. 4, 161–170.

Muller, R.H., Madder, K., Gohla, S., 2000. Solid lipid nanoparticles (SLN) for controlled drug delivery: a review of the state of the art. Eur. J. Pharm. Biopharm. 50, 161–177.

Muller, R.H., Mehnert, W., Lucks, J.S., Schwarz, C., zur Muhlen, A., Weyhers, H., Freitas, C., Ruhl, D., 1995. Solid lipid nanoparticles (SLN): an alternative colloidal carrier system for controlled drug delivery. Eur. J. Pharm. Biopharm. 41, 62–69.

Newlands, E.S., Blackledge, G.R., Slack, J.A., et al., 1992. Phase I trial of temozolomide. Br. J. Cancer 65, 287–291.

Newlands, E.S., Stevens, M.F., Wedge, S.R., et al., 1997. Temozolomide: a review of its discovery, chemical properties, pre-clinical development and clinical trials. Cancer Treat. Rev. 23, 35–61.

Yang, S.C., Lu, L.F., Cai, Y., Zhu, J.B., Liang, B.W., Yang, C.Z., 1999. Body distribution in mice of intravenously injected camptothecin solid lipid nanoparticles and targeting effect on brain. J. Control. Release 59, 299–307.